

NASA/TM–20220016943



Spectral Responses of the PACE OCI Short-Wave Infrared Detection Assembly

Jacob K. Hedelius, Kenneth J. Squire, James Q. Peterson, Branimir Blagojević, Ulrik B. Gliese, Eric T. Gorman, David K. Moser, Zakk Rhodes, Pedro Sevilla, and Gerhard Meister

November 2022

NASA STI Program ... in Profile

Since its founding, NASA has been dedicated to the advancement of aeronautics and space science. The NASA scientific and technical information (STI) program plays a key part in helping NASA maintain this important role.

The NASA STI program operates under the auspices of the Agency Chief Information Officer. It collects, organizes, provides for archiving, and disseminates NASA's STI. The NASA STI program provides access to the NTRS Registered and its public interface, the NASA Technical Reports Server, thus providing one of the largest collections of aeronautical and space science STI in the world. Results are published in both non-NASA channels and by NASA in the NASA STI Report Series, which includes the following report types:

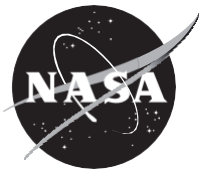
- **TECHNICAL PUBLICATION.** Reports of completed research or a major significant phase of research that present the results of NASA Programs and include extensive data or theoretical analysis. Includes compilations of significant scientific and technical data and information deemed to be of continuing reference value. NASA counterpart of peer-reviewed formal professional papers but has less stringent limitations on manuscript length and extent of graphic presentations.
- **TECHNICAL MEMORANDUM.** Scientific and technical findings that are preliminary or of specialized interest, e.g., quick release reports, working papers, and bibliographies that contain minimal annotation. Does not contain extensive analysis.
- **CONTRACTOR REPORT.** Scientific and technical findings by NASA-sponsored contractors and grantees.
- **CONFERENCE PUBLICATION.** Collected papers from scientific and technical conferences, symposia, seminars, or other meetings sponsored or co-sponsored by NASA.
- **SPECIAL PUBLICATION.** Scientific, technical, or historical information from NASA programs, projects, and missions, often concerned with subjects having substantial public interest.
- **TECHNICAL TRANSLATION.** English-language translations of foreign scientific and technical material pertinent to NASA's mission.

Specialized services also include organizing and publishing research results, distributing specialized research announcements and feeds, providing information desk and personal search support, and enabling data exchange services.

For more information about the NASA STI program, see the following:

- Access the NASA STI program home page at <http://www.sti.nasa.gov>
- E-mail your question to help@sti.nasa.gov
- Phone the NASA STI Information Desk at 757-864-9658
- Write to:
NASA STI Information Desk
Mail Stop 148
NASA Langley Research Center
Hampton, VA 23681-2199

NASA/TM–20220016943



Spectral Responses of the PACE OCI Short-Wave Infrared Detection Assembly

*Jacob K. Hedelius, Kenneth J. Squire, and James Q. Peterson
Utah State University, Logan, UT*

*Branimir Blagojević
Goddard Space Flight Center, Greenbelt, MD*

*Ulrik B. Gliese
KBR, Greenbelt, MD*

*Eric T. Gorman
Goddard Space Flight Center, Greenbelt, MD*

*David K. Moser, Zakk Rhodes, and Pedro Sevilla
Utah State University, Logan, UT*

*Gerhard Meister
Goddard Space Flight Center, Greenbelt, MD*

National Aeronautics and
Space Administration

Goddard Space Flight Center
Greenbelt, Maryland 20771

November 2022

Trade names and trademarks are used in this report for identification only. Their usage does not constitute an official endorsement, either expressed or implied, by the National Aeronautics and Space Administration.

Level of Review: This material has been technically reviewed by technical management.

Spectral Responses of the PACE OCI Short-Wave Infrared Detection Assembly

Jacob K. Hedelius, Kenneth J. Squire, James Q. Peterson, Branimir Blagojević, Ulrik B. Gliese, Eric T. Gorman, David K. Moser, Zakk Rhodes, Pedro Sevilla, and Gerhard Meister

August 12, 2022

EXECUTIVE SUMMARY

The Ocean Color Instrument (OCI) to go on the Plankton, Aerosol, Cloud, ocean Ecology (PACE) Earth-observing satellite has a Short-wave infrared (SWIR) Detection Assembly (SDA). This SDA is used to measure upwelling radiation in seven discrete bands from 940 to 2260 nm. There are redundant measurements of each band for a total of 32 physical channels, which includes optical components through to detection. The relative spectral response (RSR) is measured for each channel, which is needed when accounting for the spectral distribution of sensed radiance. From the RSR, single-value performance metrics are computed including the center wavelength, the full width at half of the maximum (FWHM), and the full width at 1% of the maximum (FW1P). Besides in-band responses, the out-of-band rejection ratio (OOBRR) is also calculated for each of the channels, which is a measure of the sensitivity outside the band of interest. We find that all 32 SDA detection channels meet the spectral response requirements at the qualification temperatures at which tests were conducted.

I. INTRODUCTION AND REQUIREMENTS

Observations from the Plankton, Aerosol, Cloud, ocean Ecology (PACE) Earth-observing satellite will provide insight into the Earth system by measuring light in bands of interest for observing the atmosphere, ocean color, and land. The Ocean Color Instrument (OCI) to go on PACE has a rotating telescope that will scan cross track in a west-to-east direction. From the telescope, light is directed to two grating spectrometers that will measure light from 340 to 890 nm at a 5 nm nominal spectral resolution. Light is also directed to a third, Short-wave infrared (SWIR) Detection Assembly (SDA) that will measure light in seven discrete bands of interest from 940 to 2260 nm (Gorman et al., 2019).

Measurements from the SDA bands are used in the retrievals of aerosol-related products and in deriving atmospheric corrections. For example, the 940 nm band, which is also used by the Aerosol Robotic Network (AERONET), is used in calculating total precipitable water vapor. The 1378 nm band, which is particularly sensitive to cirrus clouds and water vapor, may be used to correct for their effects. A list of the bands is in Table 1 (Cairns et al., 2018). Band requirements were chosen to minimize transmission losses to long-lived trace gases, while also being spectrally located in regions of interest to estimate geophysical parameters such as cloud particle sizes. Bands were also chosen based on heritage measurements (e.g., from MODIS and VIIRS) to maintain continuity.

The full width at half of the maximum (FWHM) requirement constrains the spectral width of bands, and the full width at 1% of the maximum (FW1P) requirement is that it be less than two times the nominal FWHM. Some bands have detectors configured in both high gain (HG) and

standard gain (SG) modes. To increase the signal-to-noise ratio (SNR), there are 2–8 repeats of each channel type for a total of 32 physical detection channels. These are assembled into subunits called SWIR Detection Subassemblies (SDS). There are 16 SDSs with two channels each.

Table 1. OCI SWIR band requirements and characteristics

Band (nm)	FWHM (nm)	N	OOBRR	Ocean or Atmosphere	Purpose^a
940 ± 4	45 ± 4	2	0.0075	A	Atmospheric water
1038 ± 2	75 ± 4	4	0.0075	O	Water reflectance
1250 ± 4 (SG)	30 ± 4	2	0.0075	A	Aerosols
1250 ± 4 (HG)	30 ± 4	8	0.0075	O	Water reflectance
1378 ± 2	15 ± 2	2	0.005	A	Cirrus clouds
1615 ± 10 (SG)	75 ± 10	2	0.0075	A	Aerosols
1615 ± 10 (HG)	75 ± 10	8	0.0075	O	Water reflectance
2130 ± 5	50 ± 5	2	0.0075	A	Ice vs. water clouds (w/2260)
2260 ± 10	75 ± 5	2	0.0075	Both	Ice vs. water clouds (w/2130)

^aListed purposes are examples only. SWIR bands may have multiple uses.

II. RELATIVE SPECTRAL RESPONSE

Three separate tests were conducted to ensure the detection channels of the SDA met their in-band spectral response requirements. These tests were conducted at the Utah State University Space Dynamics Laboratory (SDL) from late 2020 through early 2021—this was before full OCI system-level integration at Goddard Space Flight Center (GSFC). The output from a step-scan Fourier transform spectrometer (FTS) provided a modulated light source to the OCI detectors (Hansen et al., 2003; Tansock et al., 2015). The modulated detector response was transformed to the spectral domain, and corrections were applied to account for the spectral distribution of the FTS output. The result was normalized by dividing by the peak response to obtain the relative spectral response (RSR) with a peak response of one. The RSR is also known as the Spectral Response Function for some programs.

All three tests to characterize the RSR were conducted under thermal vacuum (TVAC) conditions. In the first of the three tests, each SDS was individually tested prior to integration into the SDA to characterize the channel’s RSR. This test was conducted at the SDS nominal optical temperature of -65°C. At this stage, out-of-band spectral measurements were also made (Sect. III). The last two RSR measurements were conducted after the SDA was assembled, and the responses of all 32 channels were characterized simultaneously. One test was conducted at a hot qualification temperature of -55°C, and another was conducted at a cold qualification temperature of -75°C.

Example spectral responses for each band are in Figure 1. From these responses, the FWHM limits were first determined, and their centers are the center wavelengths (λ_0). The FW1P limits were also empirically determined as the wavelengths where the signal first drops to less than 1% of the peak. These values are summarized for all tests and detection channels in Table 2.

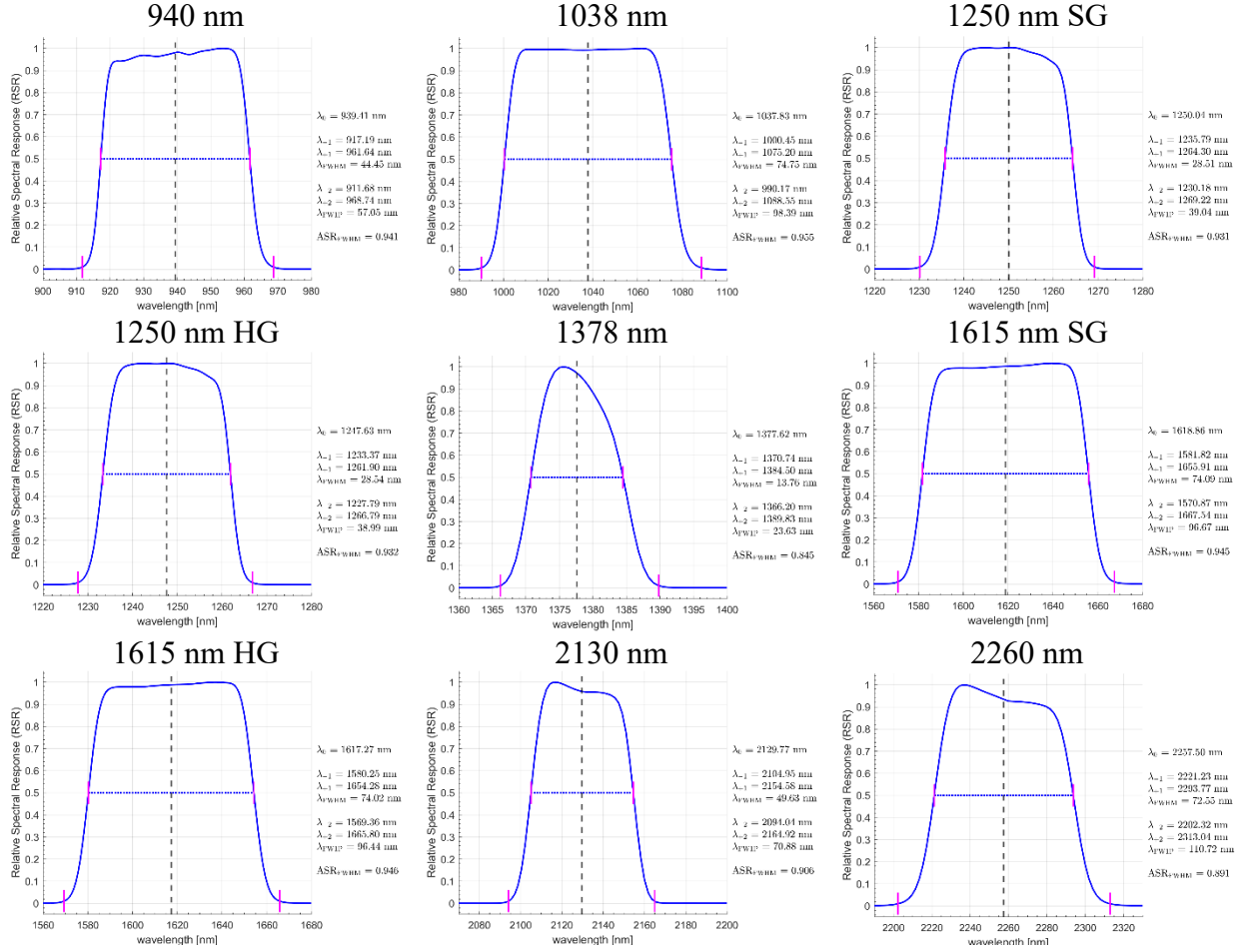


Figure 1. Representative RSRs from each of the different bands and gains. On the right of each subplot are the center wavelength (λ_0), the wavelengths marking the FWHM and their difference (λ_{-1} , λ_{+1} , and λ_{FWHM}), the wavelengths marking the FWIP and their difference (λ_{-2} , λ_{+2} , and λ_{FWIP}), and the average response across the FWHM region.

III. OUT-OF-BAND REJECTION RATIOS

The out-of-band rejection ratio (OOBRR) is a ratio of the amount of signal expected to originate from light outside the FWIP range versus the amount from within for a typical solar spectrum, which in theory is:

$$\text{OOBRR} = \frac{\int_0^{\lambda_{-2}} R_s(\lambda) d\lambda + \int_{\lambda_{+2}}^{\infty} R_s(\lambda) d\lambda}{\int_{\lambda_{-2}}^{\lambda_{+2}} R_s(\lambda) d\lambda} \quad (1)$$

where $R_s(\lambda)$ is the expected response of the system to a solar spectrum, accounting for optics and detector responses. The λ_{-2} , and λ_{+2} limits are the FWIP limits specified by the requirements. In practice we cannot integrate over all wavelengths from zero to infinity due to limits in the light source and modulated input signal, so we integrated from 800 nm on the

Table 2. RSR results summary

SDL Part Number	Optical Performance Req.			SDS Test Results			SDA Hot Qual			SDA Cold Qual		
	Center	Bandpass		Center	Bandpass		Center	Bandpass		Center	Bandpass	
	$\lambda_0 \pm \Delta\lambda$	$\lambda_{FWHM} \pm \Delta\lambda$	λ_{FWIP}	λ_0	λ_{FWHM}	λ_{FWIP}	λ_0	λ_{FWHM}	λ_{FWIP}	λ_0	λ_{FWHM}	λ_{FWIP}
303-0003-6	940 ± 4 nm	45 ± 4 nm	<90 nm	939.4	44.5	57.1	939.5	44.5	57.1	939.4	44.5	57.0
303-0003-1				939.8	44.5	57.2	939.6	44.5	57.0	939.4	44.4	57.1
303-0003-2	1250 ± 4 nm	30 ± 4 nm	<60 nm	1250.4	28.8	39.5	1250.5	28.8	39.5	1250.4	28.8	39.5
				1250.0	28.8	39.5	1250.1	28.8	39.4	1249.9	28.8	39.4
				1249.6	28.8	39.4	1249.7	28.8	39.5	1249.5	28.8	39.4
				1247.7	28.5	39.0	1247.8	28.5	39.0	1247.6	28.5	39.0
				1247.2	28.7	39.4	1247.3	28.7	39.4	1247.2	28.7	39.4
				1247.4	28.7	39.3	1247.5	28.7	39.3	1247.4	28.7	39.2
				1247.3	28.7	39.3	1247.4	28.7	39.3	1247.2	28.7	39.3
303-0003-7				1246.8	28.6	39.3	1246.9	28.7	39.3	1246.8	28.7	39.3
303-0003-3	1250 ± 4 nm	30 ± 4 nm	<60 nm	1250.1	28.5	39.1	1250.2	28.5	39.1	1250.0	28.5	39.0
				1250.0	28.8	39.4	1250.1	28.8	39.3	1249.9	28.8	39.4
303-0003-4	1038 ± 2 nm	75 ± 4 nm	<150 nm	1038.1	74.6	98.3	1038.4	74.8	98.4	1038.2	74.8	98.1
				1037.2	74.5	98.2	1037.5	74.8	98.6	1037.3	74.7	98.3
303-0003-5				1037.7	74.5	98.2	1038.0	74.8	98.5	1037.8	74.8	98.4
303-0003-8				1037.8	74.5	98.4	1038.1	74.8	98.8	1037.9	74.8	98.6
303-0003-6	1378 ± 2 nm	15 ± 2 nm	<30 nm	1378.0	14.2	23.7	1377.9	13.9	23.7	1377.7	13.9	23.7
303-0003-1				1377.9	14.2	23.7	1377.8	13.8	23.6	1377.6	13.8	23.6
303-0003-2	1615 ± 10 nm	75 ± 10 nm	<150 nm	1615.8	73.9	96.1	1616.0	73.9	96.1	1615.8	73.8	96.0
				1616.0	74.0	96.2	1616.2	74.0	96.1	1616.0	73.9	96.1
				1617.8	74.0	96.3	1617.9	74.0	96.3	1617.7	74.0	96.3
				1617.3	74.1	96.3	1617.5	74.0	96.3	1617.3	74.0	96.4
				1617.3	74.1	96.3	1617.6	74.0	96.1	1617.3	74.0	96.1
				1617.6	74.0	96.2	1617.8	74.0	96.2	1617.5	74.0	96.3
				1619.1	74.1	96.4	1619.3	74.1	96.3	1619.0	74.1	96.3
303-0003-7				1618.9	74.1	96.4	1619.0	74.0	96.3	1618.8	74.0	96.3
303-0003-3	1615 ± 10 nm	75 ± 10 nm	<150 nm	1619.4	74.0	96.3	1619.5	74.0	95.9	1619.3	74.0	95.9
				1618.9	74.1	96.3	1619.1	74.1	96.5	1618.9	74.1	96.7
303-0003-4	2130 ± 5 nm	50 ± 5 nm	<100 nm	2130.7	49.6	70.9	2130.7	49.7	71.5	2130.4	49.7	70.8
				2130.1	49.6	70.9	2130.1	49.6	71.2	2129.8	49.6	70.9
303-0003-5	2260 ± 10 nm	75 ± 5 nm	<150 nm	2257.9	72.9	109.9	2257.8	72.5	109.5	2257.5	72.5	110.7
303-0003-8				2257.9	72.7	110.1	2257.8	72.5	109.8	2257.5	72.5	109.5

low end to 2500 nm on the high end (2800 nm for bands 1615, 2130, and 2260 nm). We emphasize that the numerator is of the actual detector out-of-band (OOB) response and not just the measurement noise limit.

OOB spectra were acquired during the individual SDS tests. The response of detectors was measured with different combinations of optical filters in the light path to obtain OOB spectra. The responses of these OOB spectra were normalized to each other, and the absorption of the optical filters is accounted for. Similar spectra could be obtained by sufficiently long collects; however, since the SNR only improves with \sqrt{n} , collects would need to be orders of magnitude longer.

Merged spectra were then created by stitching the SDS in-band spectra (Sect. II) within the FW1P region together with the OOB spectra for areas outside of the FW1P. These merged spectra were used to calculate the OOBRR following Eq. 1 and using a typical solar spectrum. By merging spectra collected with different combinations of optical filters, we save testing time while still measuring the OOBRR of the detector response rather than just the ratio of the in-band response to the OOB noise. The OOBRR results are summarized in Table 3. To obtain SDA-level merged spectra, SDA in-band spectra were combined with SDS OOB spectra.

Table 3. OOBRR values

Detector λ (nm) & SDS#	SDS	SDA Hot Q.	SDA Cold Q.
940 (01)	0.0003	0.0003	0.0003
940 (02)	0.00003	0.0003	0.0003
1250 HG (03)	0.0012	0.0012	0.0012
1250 HG (04)	0.0007	0.0007	0.0007
1250 HG (05)	0.0014	0.0012	0.0032
1250 HG (06)	0.0006	0.0013	0.0032
1250 HG (07)	0.0033	0.0013	0.0032
1250 HG (08)	0.0013	0.0009	0.0016
1250 HG (09)	0.0012	0.0011	0.0018
1250 HG (10)	0.0007	0.0009	0.0015
1250 SG (11)	0.0007	0.0007	0.0011
1250 SG (12)	0.0006	0.0006	0.0006
1038 (13)	0.0002	0.0002	0.0002
1038 (14)	0.0002	0.0002	0.0002
1038 (15)	0.0001	0.0001	0.0001
1038 (16)	0.0001	0.0001	0.0001
1378 (01)	0.0029	0.0029	0.0003
1378 (02)	0.0032	0.0018	0.0003
1615 HG (03)	0.0006	0.0006	0.0012
1615 HG (04)	0.0004	0.0004	0.0007
1615 HG (05)	0.0002	0.0002	0.0032
1615 HG (06)	0.0002	0.0002	0.0032
1615 HG (07)	0.0003	0.0004	0.0032
1615 HG (08)	0.0012	0.0012	0.0016
1615 HG (09)	0.0008	0.0008	0.0018
1615 HG (10)	0.0001	0.0001	0.0015
1615 SG (11)	0.0002	0.0002	0.0011
1615 SG (12)	0.0004	0.0004	0.0006
2130 (13)	0.0005	0.0005	0.0002
2130 (14)	0.0004	0.0004	0.0002
2260 (15)	0.0004	0.0004	0.0001
2260 (16)	0.0006	0.0007	0.0001

IV. AVERAGED RESULTS

Multiple detection channels of the same band and gain provide redundancy and increase the total SNR for that channel. Unweighted averages of the spectra acquired during SDS-level testing and described in Section III were found along with their standard deviations. These spectra are shown in Fig. 2 separated by high gain and standard gain bands. From these average spectra, we calculate the spectral parameters λ_0 , FWHM, and FW1P described in Section II, as well as the OOBRR described in Section III. Spectral parameters from these averaged spectra are tabulated in Table 4.

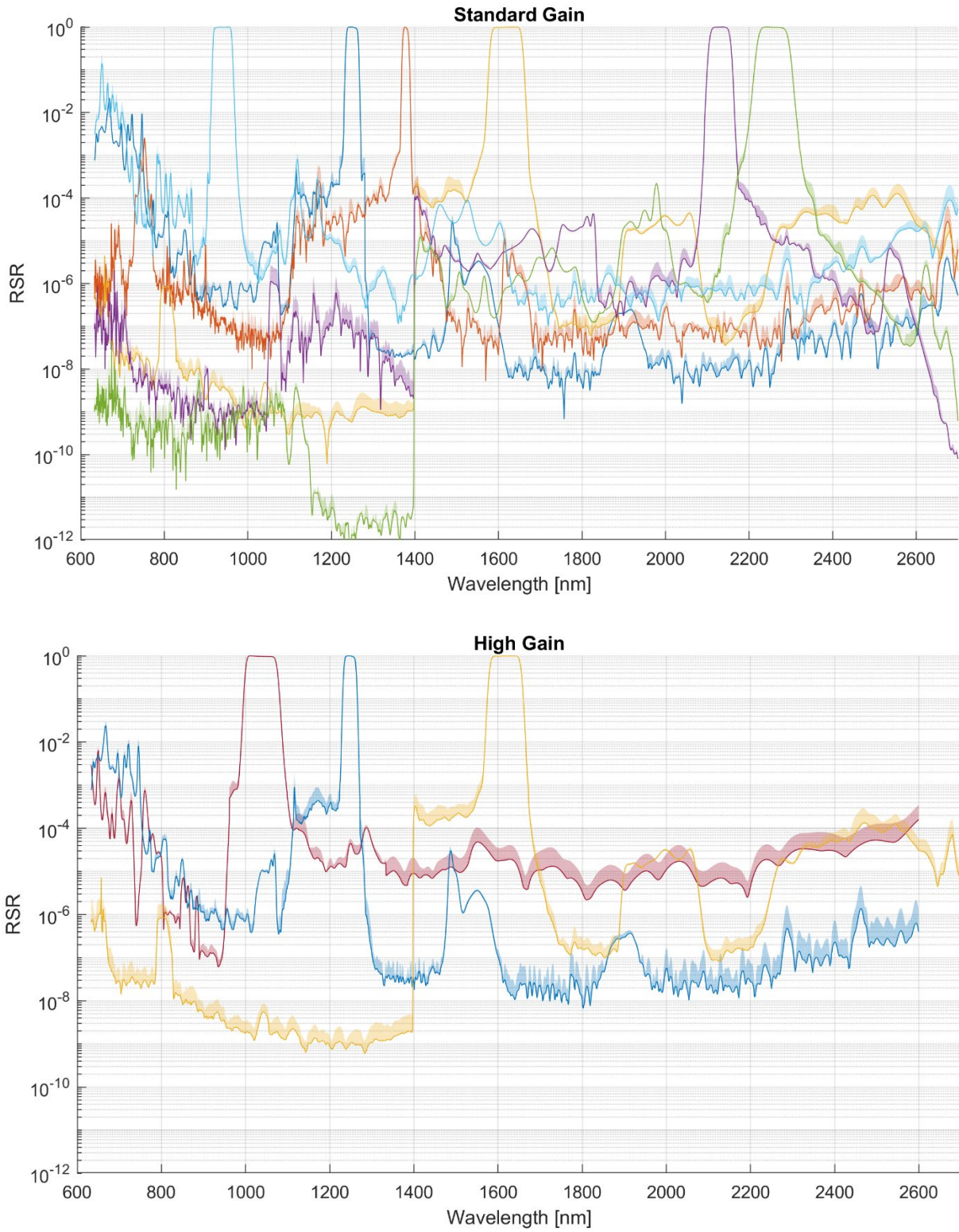


Figure 2. Averaged RSR and OOB merged spectra for each band and gain. Shaded regions represent $+1\sigma$.

Table 4. SDS spectral parameters from averaged spectra.

Band (nm) / gain	Center λ (nm)	λ_{FWHM}	λ_{FW1P}	OOBRR ($\times 10^4$)
940	939.6	44.5	57.2	2.4
1038	1037.7	74.5	98.1	1.5
1250 HG	1248.2	28.7	40.8	13.0
1250 SG	1250.0	28.7	39.2	6.2
1378	1378.0	14.2	23.6	25.2
1615 HG	1617.5	74.0	96.7	4.8
1615 SG	1619.1	74.1	96.4	3.3
2130	2130.4	49.6	70.9	4.5
2260	2257.9	72.8	110.0	5.1

V. DISCUSSIONS AND SUMMARY

The spectral responses of the 32 detection channels for the PACE OCI SDA are characterized for both their in-band and out-of-band responses. Tests were conducted first on each fully assembled SDS individually and then on all SDSs simultaneously after they were assembled into the SDA. SDS testing was performed at nominal operating temperature (-65°C), and SDS testing was performed at cold qualification (-75°C) and hot qualification (-55°C) temperatures. In-band responses are summarized by the center wavelengths, FWHM, and FW1P. We find all in-band metrics meet the OCI program requirements. OOBRRs, or ratios between out-of-band responses to in-band responses for a typical solar spectrum, are also summarized for all 32 channels. All OOBRRs are also within specifications.

Despite meeting OCI program requirements, the standard deviation of center wavelengths is greater than 0.5 nm for the sets of high gain bands 1250 nm and 1615 nm (Table 2). Similar missions in the future may consider adopting requirements for the range-of-center wavelengths among equivalent bands and gains. In addition to the variation in λ_0 among similar physical detectors within a single test, there are also systematic differences in λ_0 for the same detectors at different temperatures (Table 2). Hot qualification λ_0 values are 0.19 ± 0.05 nm larger than values at cold qualification temperatures, for an average rate of 7.6×10^{-3} nm/K. This difference has a wavelength dependence and is approximately 0.13 nm for the 940 nm band increasing nearly linearly with wavelength to 0.31 nm for the 2260 nm band. This variation with temperature is a fundamental behavior of thin film narrow bandpasses, such as those used for the SDA (Stolberg-Rohr and Hawkins, 2015).

Note that the RSRs measured at SDA level are different from the OCI system-level RSRs. The main difference is that OCI directs light of wavelengths below 900 nm to the grating spectrometers. The in-band RSR parameters presented here are not significantly affected by this difference, but it is important for the below 900 nm OOB RSR.

VI. AUTHOR CONTRIBUTIONS AND ACKNOWLEDGEMENTS

JKH performed the formal analysis, created the visualizations, and wrote the initial draft. JKH, KJS, JQP, and GM reviewed and edited the paper. PS created the software used for data acquisition. KJS and DKM collected data used in analysis. ZR designed the SDA electronics. UBG was involved in SDA optical design, and BB supported the SDA optical filter design. GM and ETG secured funding and provided project administration.

We thank the following for their contributions to this work: Paul Fluckiger for assembling the SDA, James A. Champagne for leading overall SDA optical design, Gabriel Loftus for leading SDA project management at the Space Dynamics Laboratory, and Hannah Brailsford for technical review and editing.

We acknowledge contract funding through the NASA GSFC PACE program.

VII. COMPANION PRESENTATION

This work was also presented at SPIE Optics+Photonics 24 August 2022 (paper 12232-38).

VIII. REFERENCES

Cairns, B., and A. Ibrahim (2018), Analysis of PACE OCI SWIR Bands, in PACE Technical Report Series, Volume 7: Ocean Color Instrument (OCI) Concept Design Studies (NASA/TM-2018 – 2018-219027/ Vol. 7), edited by I. Cetinić, C. R. McClain, and P. J. Werdell, NASA Goddard Space Flight Space Center Greenbelt, MD.

<https://ntrs.nasa.gov/api/citations/20190001627/downloads/20190001627.pdf>.

Gorman, E. T., D. A. Kubalak, D. Patel, A. Dress, D.B. Mott, G. Meister, and P.J. Werdell (2019), The NASA Plankton, Aerosol, Cloud, ocean Ecosystem (PACE) mission: an emerging era of global, hyperspectral Earth system remote sensing, in: SPIE Proceedings Volume 11151, Sensors, Systems, and Next-Generation Satellites XXIII, Strasbourg, France, 10 October 2019, <https://doi.org/10.1117/12.2537146>.

Hansen, S., J. Peterson, R. Esplin, and J. Tansock (2003), Component level prediction versus system level measurement of SABER relative spectral response, *Int. J. Remote Sens.*, 24:2, 389–402, <https://doi.org/10.1080/01431160304968>.

Tansock, J., D. Bancroft, J. Butler, C. Cao, R. Dalta, S. Hansen, D. Helder, R. Kacker, H. Latvakoski, M. Mlynczak, T. Murdock, J. Peterson, D. Pollock, R. Russell, D. Scott, J. Seamons, T. Stone, A. Thurgood, R. Williams, X.J. Xiong, and H. Yoon (2015), NISTHB 157 Guidelines for Radiometric Calibration of Electro-Optical Instruments for Remote Sensing, <https://dx.doi.org/10.6028/NIST.HB.157>.

Stolberg-Rohr, T. and G. J. Hawkins (2015), Spectral design of temperature-invariant narrow bandpass filters for the mid-infrared, *Opt. Express* 23, 580–596, <https://doi.org/10.1364/OE.23.000580>.